Heavy Group 14 1,(n+2)-Dimetallabicyclo[*n.n.n*]alkanes and 1,(n+2)-Dimetalla[*n.n.n*]propellanes: Are They All Realistic Synthetic Targets?

Niclas Sandström and Henrik Ottosson*[a]

Abstract: [*n.n.n*]Propellanes and bicyclo[*n.n.n*]alkanes ($1 \leq n \leq 3$) in which the bridgeheads and bridges are composed of different Group 14 elements will not be ideal homologues of the all-carbon propellanes and bicycloalkanes. We used quantum-chemical calculations to conclude which of these could possibly be stable at ambient temperature. Structures, strain, and dimerization energies of [*n.n.n*]propellanes and bicyclo[*n.n.n*]alkanes with C-based tethers and with Si, Ge, or Sn at the bridgehead positions were calculated. The aptitude to add water was probed in selected cases. Comparisons were made with the analogous all-C propellanes and bicycloalkanes. All heavy 1,(n+2)-dimetallabicyclo[*n.n.n*]alkanes should be thermally stable and suitable synthetic targets, even though the moisture sensitivity of 1,3-dimetallabicyclo[1.1.1]pentanes increases as Group 14 is descended. For 1,(n+2)-dimetalla[*n.n.n*]propellanes, the incompatibility between the tether and M–M bond lengths impacts strongly on structure and stability. At ambient temperature 1,3-disila[1.1.1]propellanes should oligomerize instantly upon formation, whereas 1,3-digerma- and 1,3-distanna[1.1.1]propellanes should be less prone to oligomerize and possibly isolable. The 1,4-dimetalla[2.2.2]propellanes with M = Si–Sn have biradical ground states and can presumably only be observed under inert conditions at cryogenic temperatures. Finally, we predict that 1,5-disila[3.3.3]propellane will be persistent at ambient temperature, but 1,5-distanna[3.3.3]propellane should rapidly oligomerize.

Keywords: cage compounds • Group 14 elements • oligomerization • quantum-chemical calculations • strained molecules

Introduction

Recently, Kira et al. prepared the first 1,3-disilabicyclo[1.1.0]butane,[1] a compound with a partially inverted Si–Si bond.[2] A fully inverted Si–Si bond is found in 1,3-disila[1.1.1]propellane, a species that hitherto has not been made, even though the parent all-carbon [1.1.1]propellane and a pentastanna[1.1.1]propellane derivative, that is, ligand-stabilized cluster compounds with "naked" Group 14 atoms,[3] were prepared by Wiberg and Walker[4] and Sita et al.[5] Of the larger synthesized [*n.n.n*]propellanes, only 3,7,10-trichalcogenaoctasila[3.3.3]propellanes[6] and a 1,6-disila[4.4.4]propellane[7] have heavy Group 14 bridgehead atoms. The bridgehead Si atoms in the former species are not inverted, but the Si-Si-C angles (105.9°) in the latter reveal a trend towards inversion.[7b]

With shorter tethers the strain will increase, and if 1,(n+2)-dimetalla[*n.n.n*]propellanes with C-, N-, or O-based tethers with $n = 3$ were to be made their M–M (M = Si, Ge, or Sn) bonds could break with formation of biradicals.[8] M–M bond breakage in small polyhedral compounds with three-membered rings is facile,[9] and Kutzelnigg concluded that Si, Ge, Sn, and Pb prefer four-membered over three-membered rings due to an inability to properly form hybrid orbitals.[10] Such M–M bond breakage followed by oligomerization would yield heavy-core staffanes,[11] that is, oligomers of 1,3-dimetalla[1.1.1]propellanes, that could have interesting electronic and optical properties, since the M atoms in these chains may couple. Due to possibly useful optoelectronic properties of the oligomers, the stabilities of 1,(n+2)-dimetallabicyclo[*n.n.n*]alkanes are also of interest, as these represent the oligomer repeat units. Through-space interactions in bicyclo[1.1.1]pentane and in staffanes have been observed,[12–20] and stronger interactions in heavy-core staffanes can be envisioned.

---

[a] N. Sandström, Dr. H. Ottosson
Department of Chemistry, Organic Chemistry
Box 599, Uppsala University, 751 24 Uppsala (Sweden)
Fax: (+46) 18-471-3818
E-mail: henrik.ottosson@kemi.uu.se

Supporting information for this article is available on the WWW under http://www.chemeurj.org/ or from the author.

DOI: 10.1002/chem.200500049

However, the selection of reported heavy bicyclo[*n.n.n*]alkanes is limited. Bicyclo[1.1.1]pentanes and bicyclo[2.2.2]octanes in which all C atoms have been replaced by heavier elements have been made,[5b,21–26] and those with all C atoms replaced by Si or Sn show structural homology to the all-C compounds. However, with different Group 14 elements in tethers and at bridgeheads, these species cannot display such homology. The 9,10-dimetallatriptycenes of Takahashi et al.[27] and Bickelhaupt et al.[28] are the bicyclic species with the shortest C-based tethers linking bridgehead Si, Ge, and Sn atoms. This near lack of Group 14 1,(n+2)-dimetalla[*n.n.n*]propellanes and 1,(n+2)-dimetallabicyclo[*n.n.n*]alkanes with $n=3$ (Scheme 1) led us to probe computationally which of these are realistic synthetic targets. Allen et al. earlier computed structures and strain energies of [1.1.1]propellanes and bicyclo[1.1.1]pentanes with some or all C atoms exchanged for Si,[29] and concluded that these species will not be prone to polymerize and thus represent good candidates for synthesis. We probed the structures of 1,(n+2)-dimetalla[*n.n.n*]propellanes and 1,(n+2)-dimetallabicyclo[*n.n.n*]alkanes ($n=1$–3 and M = C–Sn) and found trends in strain and stability against oligomerization that, in part, contradict earlier findings.

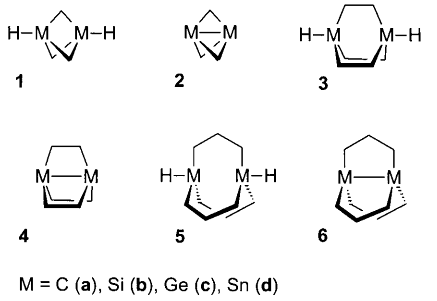

Scheme 1. 1,(n+2)-Dimetallabicyclo[*n.n.n*]alkanes and 1,(n+2)-dimetalla[*n.n.n*]propellanes investigated in this study.

The all-C bicyclo[*n.n.n*]alkanes and [*n.n.n*]propellanes ($n=1$–3) were prepared earlier,[30–35] but their stabilities vary greatly. Bicyclo[*n.n.n*]alkanes and the [3.3.3]propellane are inert, but most [2.2.2]- and [1.1.1]propellanes polymerize and/or rearrange, the exceptions being the fluorinated [2.2.2]propellanes of Lemal et al.[36] One could reason that if a heavy dimetalla[*n.n.n*]propellane or dimetallabicyclo[*n.n.n*]alkane is less strained than its all-C analogue, it will be at least as stable as the latter, and this could be particularly true if the strain difference of a heavy propellane/bicycloalkane pair is smaller than the strain difference of the analogous all-C pair. However, such a comparison of the all-C with the heavier systems is oversimplified, as the stability of the propellane depends on the relative M–M bond strengths of the propellane and the oligomer. High M–M bond polarizabilities of the heavy propellanes should also facilitate their oligomerization. We analyzed these and other issues using computations, with the aim of rationalizing which species can possibly exist at ambient temperature.

Computational Methods

All calculations were done with the Gaussian 03 program package.[37] The first optimizations were done at the B3LYP hybrid density functional theory level[38] with the 6-31G(d) basis set for C and H[39] and the LANL2DZ relativistic effective core potential (ECP) of Hay and Wadt for Si, Ge, and Sn,[40] extended with the d-type polarization functions of Sunderlin et al., optimized for B3LYP and MP2 calculations.[41] We write this basis set combination as 6-31G(d)(LANL2DZd). The stationary points were subjected to frequency calculations to check their characters as minima or saddle points. The structures that correspond to minima were further optimized at the B3LYP level with the cc-pVTZ basis set for C, Si, and H, and the SDB relativistic ECP of Martin and Sundermann for Ge and Sn.[42] This basis set combination is written here as cc-pVTZ(SDB). Geometry optimizations of all compounds were also performed at the MP2 level with 6-31G(d)(LANL2DZd) and cc-pVTZ-(SDB) for 1,3-dimetalla[1.1.1]propellanes and 1,3-dimetallabicyclo[1.1.1]pentanes. For the last two compound classes we also performed CCSD(T)/cc-pVTZ(SDB)//MP2/cc-pVTZ(SDB) calculations to evaluate the quality of strain energies calculated with B3LYP and MP2.

The stability of the Kohn–Sham solutions was checked for the 1,(n+2)-dimetalla[*n.n.n*]propellanes and their biradical oligomers.[43] The Kohn–Sham solutions were in all cases found to be stable. Biradicals were calculated with CASSCF, unrestricted B3LYP, spin-projected UMP2 (PMP2), and Brueckner doubles with perturbative triples excitations [BD(T)]. The norm of amplitudes of the single excitations (T_1 diagnostics) in the CCSD wavefunctions was calculated for systems with possible multiconfigurational character.[44]

The nature of the bonding interaction was investigated with the help of the calculated electron density distribution $\rho(r_b)$ at the bond critical points r_b by using the AIM2000 program.[45,46] Static dipole polarizabilities of the 1,3- and 1,5-dimetalla[*n.n.n*]propellanes were calculated at the B3LYP level with the 6-31G(d)(LANL2DZd) and cc-pVTZ(SDB) basis sets. These calculations were performed to estimate how the M–M long-axis polarizability component α_{zz} of a compound class scales when Group 14 is descended, and not to provide the most precise values.

Results and Discussion

We first probed the quality of the strain energies calculated with the inexpensive methods against those from high-level CCSD(T) calculations on the two smallest systems. Results for a 1,(n+2)-dimetallabicyclo[*n.n.n*]alkane are presented before those of the analogous 1,(n+2)-dimetalla[*n.n.n*]propellane, as the strain and geometry of the former is helpful when discussing the oligomerization aptitude of the latter. When going down Group 14 systems **1**–**6** show different trends in strain. The strain is connected to geometrical distortions, and the reference distances for M–M and C–M single bonds were taken from $H_3M{-}MH_3$ and $H_3C{-}MH_3$ (Table 1). The strains of **2**, **4**, and **6** were also compared to those of 1,2-dimetallacycloalkanes **7**–**9** (Scheme 2 and Table 2). We estimated strain energies by means of homodesmotic reactions, which involve equal numbers of differently hybridized atoms in reactants and products (Scheme 3).[47] Earlier computations show that homodesmotic reactions best describe strain energies in three-membered cyclic heterosilanes.[48]

1,3-Dimetallabicyclo[1.1.1]pentanes (1): The strain energy of **1a** at the B3LYP/cc-pVTZ level is 65.4 kcal mol^{-1}, and a

Table 1. M–M′ bond lengths of $H_3M–M'H_3$ compounds.

Compound	M–M′ distance [Å] MP2/6-31G(d) (LANL2DZd)	B3LYP/cc-pVTZ (SDB)
CH_3CH_3	1.526	1.527
SiH_3SiH_3	2.322	2.354
GeH_3GeH_3	2.463	2.461
SnH_3SnH_3	2.822	2.836
CH_3SiH_3	1.882	1.884
CH_3GeH_3	1.965	1.973
CH_3SnH_3	2.142	2.163

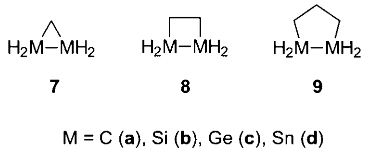

Scheme 2. 1,2-Dimetallacycloalkanes.

Table 2. Homodesmotic strain energies of 1,2-dimetallacycloalkanes.[a]

Compound	Symm.	MP2/ 6-31G(d) (LANL2DZd)	B3LYP/ cc-pVTZ (SDB)
cyclopropane (**7a**)	D_{3h}	30.3	25.8
1,2-disilacyclopropane (**7b**)	C_{2v}	41.1	37.2
1,2-digermacyclopropane (**7c**)	C_{2v}	41.5	37.9
1,2-distannacyclopropane (**7d**)	C_{2v}	40.9	36.8
cyclobutane (**8a**)	D_{2d}	28.0	25.3
1,2-disilacyclobutane (**8b**)	C_2	22.3	20.3
1,2-digermacyclobutane (**8c**)	C_2	20.9	19.4
1,2-distannacyclobutane (**8d**)	C_2	19.0	18.1
cyclopentane (**9a**)	C_2	7.7	6.5
1,2-disilacyclopentane (**9b**)	C_{2v}	6.2	6.1
1,2-digermacyclopentane (**9c**)	C_{2v}	6.0	5.7
1,2-distannacyclopentane (**9d**)	C_{2v}	7.0	6.8

[a] Energies in kcal mol^{-1} calculated in accordance with Equation (3) (Scheme 3).

value of 61.3 kcal mol^{-1} is computed with B3LYP/6-311G(d) zero-point energy (ZPE) correction. This is lower than the measured value (66.6 kcal mol^{-1}),[49] and better agreements are obtained at the CCSD(T)/cc-pVTZ//MP2/cc-pVTZ, MP2/cc-pVTZ, and MP2/6-31G(d) levels (64.9, 64.1, and 65.2 kcal mol^{-1}, respectively, with MP2/6-31G(d) ZPE corrections). Even though **1a** is highly strained it is thermally stable up to 300 °C, above which it rearranges to 1,4-pentadiene.[31] When comparing strain energies of **1a**–**1d** calculated with the inexpensive MP2 and B3LYP methods with those from CCSD(T)/cc-pVTZ(SDB)//MP2/cc-pVTZ(SDB), MP2 produces the best agreement (Figure 1), even though B3LYP properly describes the trend and magnitude of the change in strain.

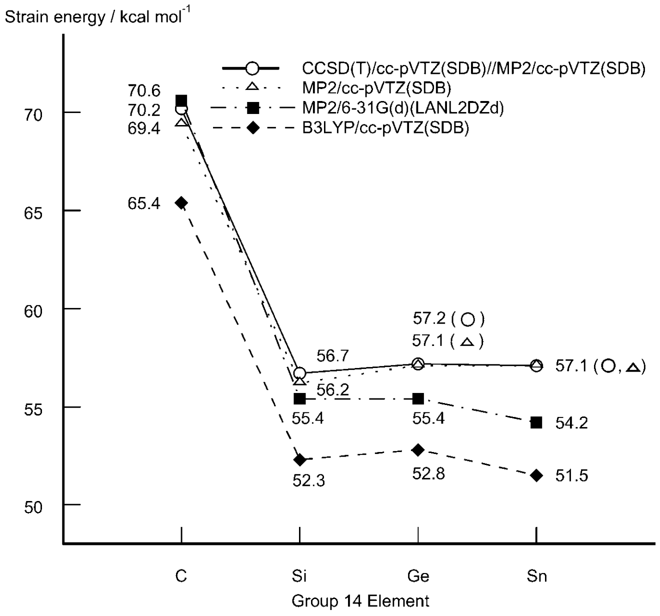

Figure 1. Homodesmotic strain energies of **1a**–**1d** at the CCSD(T)/cc-pVTZ(SDB)//MP2/cc-pVTZ(SDB), MP2/cc-pVTZ(SDB), B3LYP/cc-pVTZ(SDB), and MP2/6-31G(d)(LANL2DZd) levels.

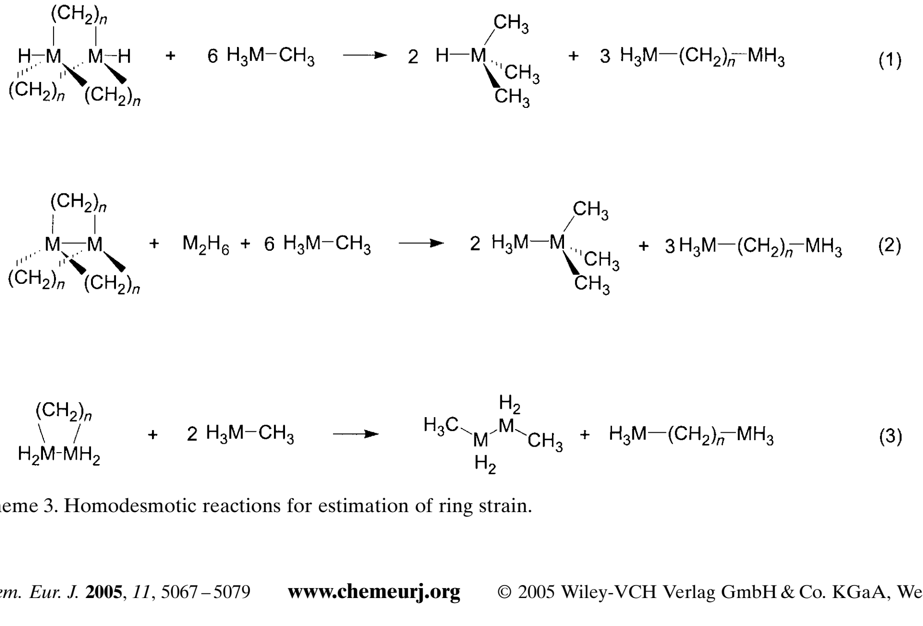

Scheme 3. Homodesmotic reactions for estimation of ring strain.

Since **1b**–**1d** are less strained than **1a** by 12–15 kcal mol^{-1} (Figure 1), they should be thermally stable at ambient temperature. The stabilities of the previously prepared bicyclo[1.1.1]pentasilane,[25] bicyclo[1.1.1]pentastannane,[5,24] as well as 2,4,5-trithia- and 2,4,5-triselena-1,3-disilabicyclo-[1.1.1]pentanes,[26] support this conclusion. The Si-containing bicyclo[1.1.1]pentanes are stable at their melting points (175–220 °C), even though 2,4,5-trithia- and 2,4,5-triselena-1,3-disilabicyclo[1.1.1]-

pentane[12,26] degrade upon exposure to moisture. Moreover, **1b** is less strained than 1,3-disilabicyclo[1.1.0]butane (MP2/6-31G(d)(LANL2DZd) strain energies are 55.4 and 63.9 kcal mol^{-1}, respectively), and the 1,3-disilabicyclo[1.1.0]butane of Kira et al. is thermally stable at its melting point of 175–177 °C.[1] Its sensitivity to oxygen and moisture should stem from the partially inverted Si–Si bond, accessible to, for example, hydrolysis. Moreover, **1a** rearranges to 1,4-pentadiene above 300 °C in a process that is exothermic by 15.4 kcal mol^{-1} at the MP2/6-31G(d) level, but similar processes will not occur for **1b**–**1d**, as the 2,4-dimetalla-1,4-pentadienes are exothermic by 40.5–48.6 kcal mol^{-1}.

The geometries of the individual **1b**–**1d** are similar at the three computational levels. Good agreement is also found between our computed structures of **1a** and the electron diffraction structure,[50] the only deviation being the distance between the two bridgehead carbons C_{bh}–C_{bh}, which differs by 0.03 Å. The nonbonded C_{bh}–C_{bh} distance in **1a** is about 0.35 Å longer than the C–C bond length in ethane (Figure 2 and Table 1), but the M–M distances of **1b**–**1d** are within 0.06 Å of the M–M bond lengths of H_3M–MH_3. Hence, the coupling between the two bridgehead atoms should be stronger in the heavy congeners than in **1a**, for which coupling between the two bridgehead C atoms was detected by a range of experimental and computational techniques.[12–20]

The decrease in strain as one goes from **1a** to **1d** is intriguing, as the M–M distances become much shorter than the optimal van der Waals distances.[51] Similar to the conclusions of Nagase and Kudo for O and S bridges,[52] the methylene bridges should withdraw electron density from the M atoms and allow the bridgehead atoms to come close in **1b**–**1d** without causing van der Waals repulsion. The C-M-C angles of **1b**–**1d** are about 90°, and since Si–Sn are less prone than C to hybridize,[10] one could also argue that these atoms are better suited than C for bridgehead positions. However, natural bond orbital analyses at the B3LYP/cc-pVTZ(SDB) level reveal that the orbitals used by the M atoms to bind the methylene tethers are sp^3-hybridized in all four compounds. On the other hand, the σ(M–C) bond orbitals are equally composed of the two sp^3(C) orbitals in **1a** but of only about 25 % of the sp^3(M) orbitals in **1b**–**1d**, which supports the conclusion of Nagase and Kudo. Simultaneously, the shortest distance between the methylene tethers increases from 2.3 to about 2.6 Å on going from **1a** to **1b**.

Draining electron density from the M atoms makes them electrophilic and vulnerable to nucleophilic attack by, for example, water (Figure 3). At the B3LYP/6-31G(d)-(LANL2DZd) level the transition states for 1,3-dimetallacyclobutane formation are found at energies of 22.3 (**1b**), 20.4 (**1c**), and 10.1 kcal mol^{-1} (**1d**) relative to the reactants, and the MP2/6-31G(d)(LANL2DZd) energies are similar (27.0, 25.6, and 14.0 kcal mol^{-1}). The barriers should be lower if

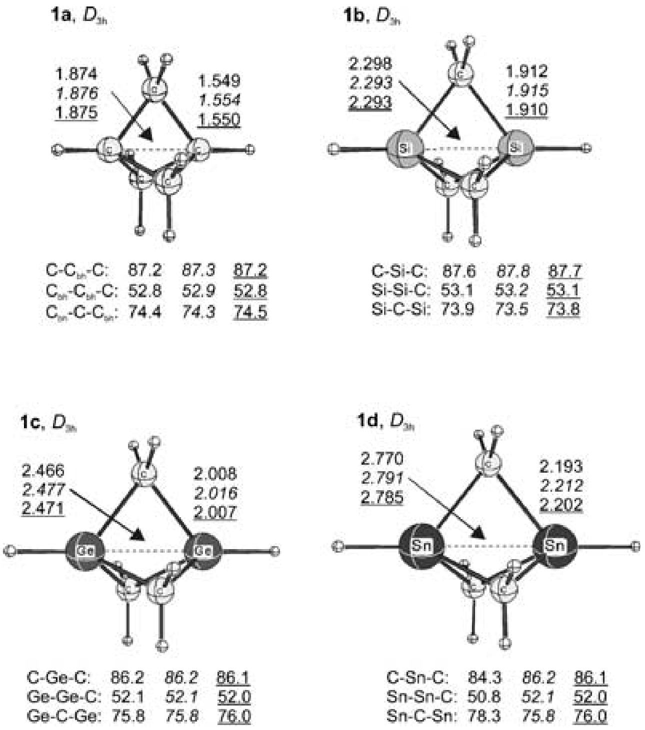

Figure 2. Optimal geometries of **1a**–**1d** at the MP2/6-31G(d)-(LANL2DZd) (normal print), B3LYP/cc-pVTZ(SDB) (italics), and MP2/cc-pVTZ(SDB) (underlined) levels.

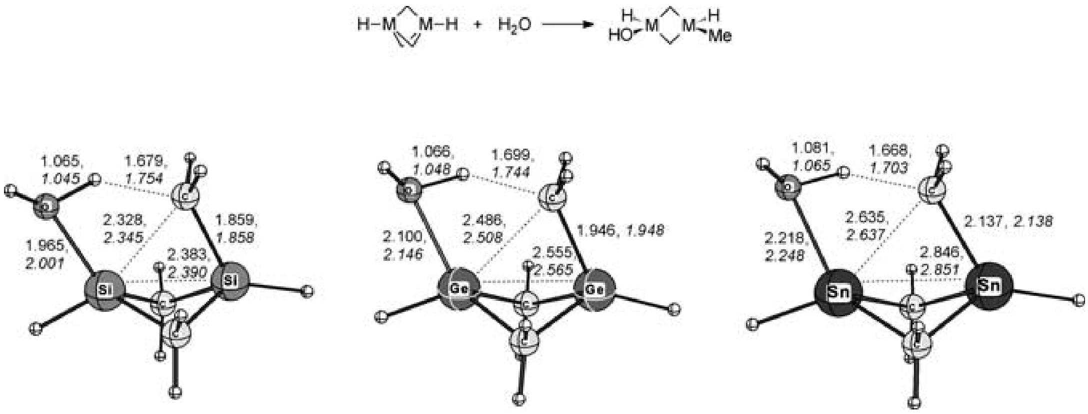

Figure 3. Transition state structures for addition of H_2O to **1b**–**1d**, calculated at the MP2/6-31G(d)(LANL2DZd) (normal print) and B3LYP/6-31G(d)-(LANL2DZd) (italics) levels. Distances in Å.

several H_2O molecules assist in M−C bond breakage, that is, **1d** will be rapidly degraded when exposed to moisture, whereas **1b** and **1c** will have longer but not infinite lifetimes.

Since Si, Ge, and Sn at the bridgeheads lower the strain of 1,3-bicyclo[1.1.1]pentanes, one could ask whether these atoms also fit well at these positions in [1.1.1]propellanes.

1,3-Dimetalla[1.1.1]propellanes (2): The strain energies of **2a** are 93.3 and 104.0 kcal mol^{-1} at the B3LYP/cc-pVTZ and MP2/6-31G(d) levels, and 103 kcal mol^{-1} according to measurements.[49] The ZPE corrections at the two levels lower the energies to 88.9 and 96.0 kcal mol^{-1}. Both MP2/6-31G(d) and MP2/cc-pVTZ give good agreement for the whole series **2** when compared to CCSD(T) (Figure 4). Only for M = Sn (**2d**) is there a significant difference between MP2/6-31G(d)(LANL2DZd) and MP2/cc-pVTZ(SDB) strain energies.

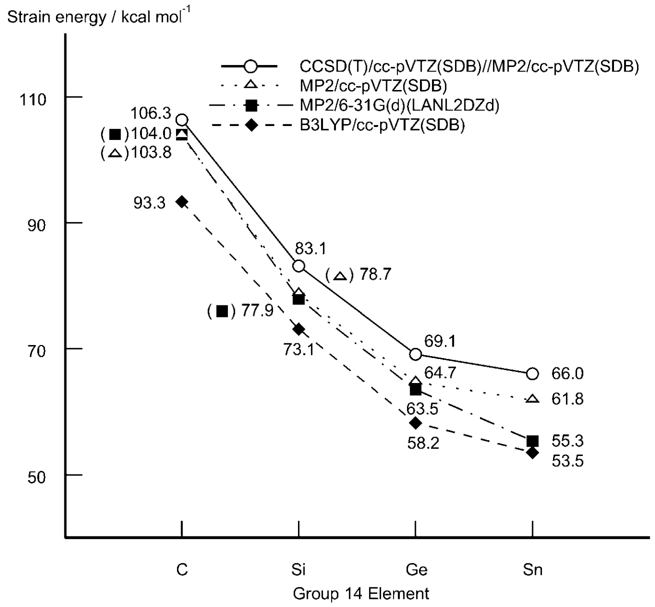

Figure 4. Homodesmotic strain energies of **2a–2d** at the CCSD(T)/cc-pVTZ(SDB)//MP2/cc-pVTZ(SDB), MP2/cc-pVTZ(SDB), B3LYP/cc-pVTZ(SDB), and MP2/6-31G(d)(LANL2DZd) levels.

When compared to three cyclopropanes (Table 2), **2a** is more strained by 13–16 kcal mol^{-1}. This species is inert in the gas phase, and only when heated to 430 °C does it rearrange to dimethylenecyclopropane,[53] although 3-methylenecyclobutene was formed at 114 °C in a process that seems to be catalyzed by the surface of the reaction vessel.[4,53] Similar to **1**, changing the bridgehead atoms from C to Si, Ge, or Sn lowers the strain. This contrasts with the trend for 1,2-dimetallacyclopropanes, and the 1,3-dimetalla[1.1.1]propellanes become gradually less strained than three 1,2-dimetallacyclopropanes by 45.3 (**2b**), 60.9 (**2c**), and 67.5 (**2d**) kcal mol^{-1} at the MP2/6-31G(d)(LANL2DZd) level. Since synthesized 1,2-disila- and 1,2-digermacyclopropanes are moderately persistent to air and moisture,[54] the 1,3-dimetalla[1.1.1]propellanes could be at least equally stable and also realistic synthetic targets.

The calculated geometries of **2a** agree with that determined by electron diffraction,[55] whereby MP2 reproduces the C_{bh}−C_{bh} bond length best. The variations in our calculated geometries of the heavy propellanes are also small (Figure 5). Interestingly, the differences between geometrical parameters of **2b–2d** and the corresponding parameters of **1b–1d** are negligible when compared to the same differences between **1a** and **2a** (Figure 2 and Figure 5). This applies particularly to the M−M distances and should have an impact on propellane oligomerization.

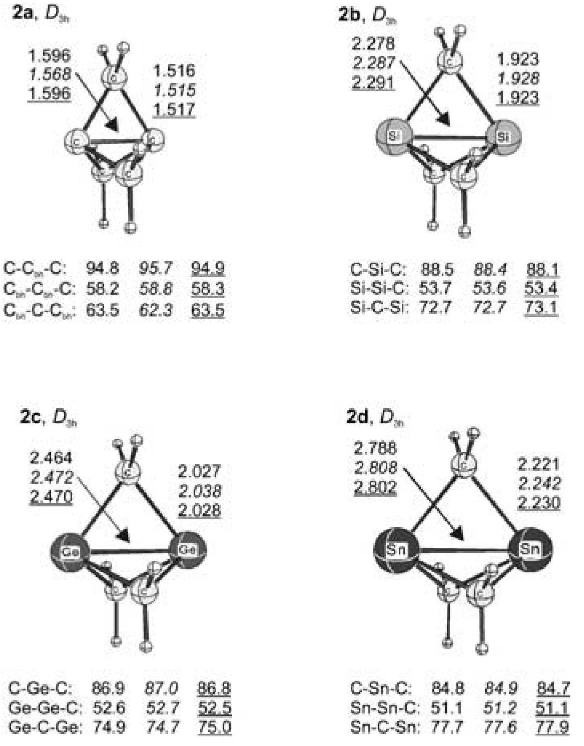

Figure 5. Optimal geometries of **2a–2d** at the MP2/6-31G(d)(LANL2DZd) (normal print), B3LYP/cc-pVTZ(SDB) (italics), and MP2/cc-pVTZ(SDB) (underlined) levels.

In contrast to the gas phase, **2a** polymerizes in solution above 0 °C.[11] It was previously found that **2a** has a low-lying triplet state due to its inverted C_{bh}−C_{bh} bond, since low-energy electron impact spectroscopy determined the vertical excitation energy to the first triplet state to be 108.3 kcal mol^{-1};[56] the same energy at the (U)B3LYP/cc-pVTZ level is 107.1 kcal mol^{-1}. Previous MP2/6-31G(d) and MP3/6-31G(d) computations estimated the adiabatic triplet state at 90.0 and 73.7 kcal mol^{-1},[63] and UB3LYP/cc-pVTZ gives 92.7 kcal mol^{-1}. With (U)BD(T)/cc-pVTZ//(U)B3LYP/cc-pVTZ as a benchmark method, the vertical and adiabatic triplet state energies are 113.8 and 96.4 kcal mol^{-1}.

We found that biradical oligomers of **2a** are of much lower relative energies than the biradical monomer, for example, the triplet biradical dimer lies 38.0 and 27.8 kcal mol^{-1} above two closed-shell monomers at the PMP2/6-31G(d) and UB3LYP/6-31G(d) levels. A singlet biradical dimer was located at 31.6, 24.8, 22.0, and 22.4 kcal mol^{-1} at the CASSCF(4,4)/6-31G(d), PMP2/6-31G(d), (U)B3LYP/6-31G(d), and (U)BD(T)/cc-pVDZ//CASSCF(4,4)/6-31G(d) levels. In the CASSCF calculations, the active space included the four σ orbitals constructed from the sp^3(Si) orbitals directed along the C_3 axis. Jug and Poredda postulated that the dimer forms on the T_1 surface by collision of two monomers followed by intersystem crossing.[57] Indeed, the singlet biradical dimer will be transient, since the transition state separating the dimer from two monomers (Figure 6) lies at 2.3 kcal mol^{-1} with CASSCF(4,4)/6-31G(d), 1.2 kcal mol^{-1} with UB3LYP/6-31G(d), and 0.3 kcal mol^{-1} with (U)BD(T)/cc-pVDZ//CASSCF(4,4)/6-31G(d). Intersystem crossing to a triplet biradical increases its lifetime and the likeliness of oligomerization.

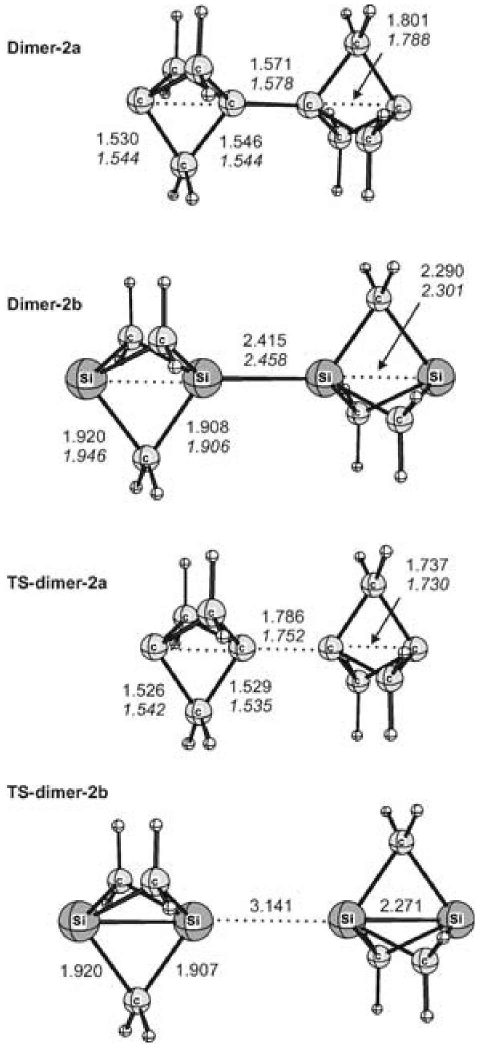

Figure 6. Optimal geometries of the singlet biradical dimers of **2a** and **2b** and the transition states for the dimerization calculated at the CASSCF-(4,4)/6-31G(d)(LANL2DZd) (normal print) and UB3LYP/6-31G(d)-(LANL2DZd) (italics) levels. Distances in Å.

Longer biradical oligomers become gradually more stable than the separated closed-shell monomers, for example, the singlet biradical tri- and tetramers of **2a** lie 12.8 and 51.4 kcal mol^{-1} below the monomers at the (U)B3LYP/6-31G(d) level. Thus, dimer formation is rate-limiting in oligomerization of **2a**, as the barrier for addition of a propellane to form the biradical trimer should be at least as low as that for splitting the dimer into two monomers. However, these longer oligomers will only form at the sufficiently high concentrations of **1a** that can be achieved in solution.

The strain difference between analogous **2** and **1** becomes smaller when descending the Group (Figure 1 and Figure 4), and since **2a** exists in the gas phase up to 114 °C and in solution up to 0 °C, one may argue that **2b**–**2d** will be equally stable.[29] The 1,3-distanna[1.1.1]propellane **2d** should be particularly stable because the biradical with a broken Sn–Sn bond is of high energy (the relaxed T_1 state lies at an energy of 47.1 kcal mol^{-1} at the (U)B3LYP/cc-pVTZ(SDB) level), and **2d** will not become significantly less strained in an oligomer with repeat units resembling **1d**. However, upon oligomerization the weak, inverted M–M bonds are converted to stronger, regular M–M bonds, and the M–M bond polarizability increases on going from **2a** to **2d** (α_{zz} = 0.67 (**2a**), 1.67 (**2b**), 1.75 (**2c**), and 2.31×10^{-23} cm^{-3} (**2d**) at the B3LYP/cc-pVTZ(SDB) level), which facilitates initialization of polymerization of heavy propellanes. The situation is critical for **2b** and **2c**, because each monomer releases strain of about 25 and about 10 kcal mol^{-1} when oligomerized. In addition, the geometries of **2b**/**2c** and **1b**/**1c** are similar, so that oligomerization requires minute nuclear motion within each monomer/repeat unit (Figures 2, 5, and 6).

Gordon et al. showed that the electron density between bridgehead M atoms in pentametalla[1.1.1]propellanes decreases as one goes from C to Sn.[58] The C_{bh}–C_{bh} bond of **2a** is already weak, with a bond order of 0.70,[59] and in **2b**–**2d** we were unable to locate (3,−1) bond critical points of the electron density along the M–M interaction lines.[45] The absence of M–M (3,−1) bond critical points could result from reversed order of the σ(M–M) and σ*(M–M) orbitals, so that the latter is HOMO for **2b**–**2d**. Such a shift occurs in [2.2.2]propellane (**4a**) when the C_{bh}–C_{bh} distance is longer than 2.3 Å,[63] but the HOMOs in all four [1.1.1]propellanes are the a_1 symmetric σ(M–M) orbitals.

Even though HOMO and LUMO of **2b**–**2d** are the σ(M–M) and σ*(M–M) orbitals, respectively, their adiabatic singlet–triplet energy gaps (ΔE_{ST} = 47.1–55.8 kcal mol^{-1} at the (U)B3LYP/cc-pVTZ(SDB) level) are much smaller than that of **2a**, whereby **2d** has the lowest ΔE_{ST}. Still, their ΔE_{ST} are larger than in O- and S-bridged 1,3-dimetalla-[1.1.1]propellanes, earlier found to have multiconfigurational character.[60] T_1 diagnostics at the CCSD/cc-pVTZ(SDB)//MP2/cc-pVTZ(SDB) level now reveal that **2a**–**2d** lack multiconfigurational character in their S_0 states.[61]

Indeed, our calculations on biradical oligomers indicate that **2b** will rapidly oligomerize. The singlet biradical dimer of **2b** is lower in energy than two separated propellanes by

5.8, 3.2, and 4.3 kcal mol^{-1} at the UB3LYP, PMP2, and CASSCF(4,4) levels with 6-31G(d)(LANL2DZd) basis set. The exothermicity increases further as oligomerization proceeds, because the singlet biradical trimer and tetramer lie 33.8 and 53.1 kcal mol^{-1} below the separated monomers at the UB3LYP/6-31G(d)(LANL2DZd) level. There is also a very low barrier to dimerization at the CASSCF(4,4)/6-31G(d)(LANL2DZd) level (3.6 kcal mol^{-1}), and at the UB3LYP level the reaction proceeds without a barrier. The forming Si–Si bond is elongated in the transition state for dimerization, and the Si–Si distance is barely changed when compared to the propellane (Figure 6). These findings oppose the conclusion of Allen et al. that **2b** will not be prone to polymerize.[29] Even though less strain is released in oligomerization of **2b** than of **2a**, all steps are exothermic and proceed over very low reaction barriers, in contrast to the oligomerization of **2a**.

The situation is more promising for **2c** and **2d**, because their biradical dimers are less stable than two monomers. We were not able to locate any singlet biradical dimers, as these dissociated into two monomers at both the CASSCF(4,4) and UB3LYP levels, but the triplet biradical dimers lie 13.4 and 17.0 kcal mol^{-1} above two 1,3-dimetalla[1.1.1]propellanes at the (U)B3LYP/6-31G(d)(LANL2DZd) level. Apparently, the relief of strain when the propellanes oligomerize, together with the energy gained upon formation of a regular M–M bond, is insufficient to compensate for the loss of two inverted M–M bonds. As oligomerization proceeds, the biradical oligomers of **2c** and **2d** become successively more stable than the separated closed-shell monomers. Nevertheless, these heavy [1.1.1]propellanes should have some short lifetimes at ambient temperature, but their thermal stabilities will be lower than that of **2a**.

As the C tethers are made longer the inverted character of the M–M bond becomes less pronounced, and this possibly leads to a lower tendency for oligomerization of 1,4-dimetalla[2.2.2]propellanes. The properties of these propellanes and the 1,4-dimetallabicyclo[2.2.2]octanes were explored next.

1,4-Dimetallabicyclo[2.2.2]octanes (3): A very modest increase in strain accompanies the change of bridgehead atom from C to Sn in 1,4-dimetallabicyclo[2.2.2]octanes (Figure 7), but none of **3b**–**3d** is overly strained and these species will be thermally stable when formed. Since the bridgehead atoms can adopt approximately tetrahedral arrangements in all of **3**, no drastic change is observed when going from **3a** to the heavier congeners, in contrast to the case of **1**. The species **3b**–**3d** are structurally similar to Group 14 9,10-dimetallatriptycenes,[27,28] compounds that are handled by standard laboratory techniques. The measured strain energy of **3a** is 7.4 kcal mol^{-1},[49] that is, 4 kcal mol^{-1} lower than our calculated values, but ZPE corrections bring us closer (9.4 kcal mol^{-1} at B3LYP/cc-pVTZ and 7.9 kcal mol^{-1} at MP2/6-31G(d) level).

The symmetries of the 1,4-dimetallabicyclo[2.2.2]octanes vary with M and computational method. Bicyclo[2.2.2]octane (**3a**) has D_{3h} symmetry with B3LYP and D_3 symmetry with MP2, whereas **3b**–**3d** are D_3-symmetric with both methods. The D_{3h}-symmetric structures of the bicyclo[2.2.2]pentanes are 0.4–6.8 kcal mol^{-1} higher in energy than the D_3-symmetric structures at the MP2/6-31G(d)(LANL2DZd) level, and the energy is highest for **3d**.

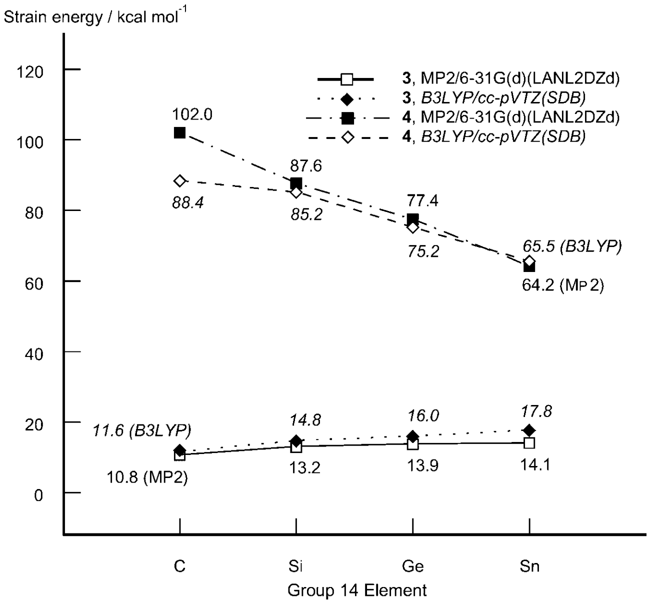

Figure 7. Homodesmotic strain energies of **3a**–**3d** and **4a**–**3d** at the B3LYP/cc-pVTZ(SDB) and MP2/6-31G(d)(LANL2DZd) levels.

The M–M distances of **3a**–**3d** are longer by 1.06, 0.65, 0.65, and 0.50 Å, respectively, when compared to the M–M bond lengths of H_3M–MH_3 (Figure 8 and Table 2), but shorter than the sum of the van der Waals radii.[51] However, the increase in strain when going from **3a** to **3d** does not affect C–C bonds and M-C-C angles, but rather the torsion within the ethylene linkers, which indicates increased eclipsing strain due to repulsive interaction between the filled σ(M–C) bond orbitals (Figure 8). When descending the Group, the σ(M–C) orbitals gradually shift to the C end. Natural bond orbital analysis of **3d** at the B3LYP/cc-pVTZ(SDB) level shows that 72.5 % of the σ(Sn-C) bond orbital is composed of sp^3(C) and 27.5 % of sp^3(Sn), whereas the σ(C_{bh}–C) orbital in **3a** is composed of 49.7 % sp^3(C_{bh}) and 50.3 % of sp^3(C) of the C atom of the ethylene linker. However, Fock matrix element deletions indicate that additional orbital interactions are also important for the observation that **3d** has the largest energy difference between the D_{3h}- and D_3-symmetric structures.

Since the strain increases on going from **3a** to **3d**, one could assume a similar rise in strain and a lower stability of the 1,4-dimetalla[2.2.2]propellanes. Conversely, heavier 1,4-dimetalla[2.2.2]propellanes will have less inverted M atoms than 1,3-dimetalla[1.1.1]propellanes.

1,4-Dimetalla[2.2.2]propellanes (4): Similar to the 1,4-dimetallabicyclo[2.2.2]alkanes, the all-C [2.2.2]propellane **4a** is D_{3h}-symmetric with B3LYP and D_3 symmetric with MP2, whereas **4b**–**4d** are D_3-symmetric. However, the major dif-

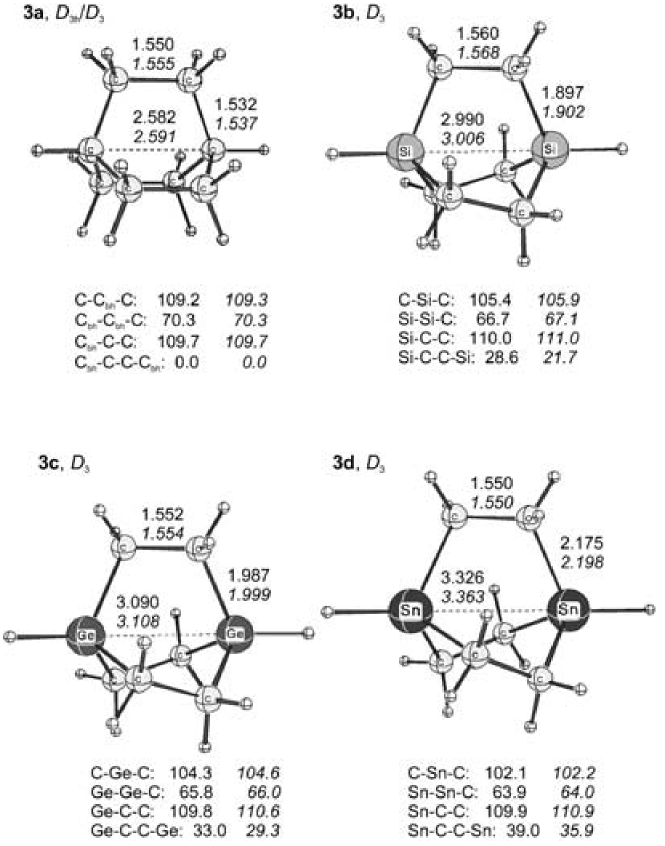

Figure 8. Optimal geometries of **3a–3d** at the MP2/6-31G(d)(LANL2DZd) (normal print) and B3LYP/cc-pVTZ(SDB) (italics) levels.

ference among the 1,4-dimetalla[2.2.2]propellanes is that **4a** is a closed-shell species, whereas **4b–4d** are biradicals without M–M bonds.

The ring strain of **4a** at the B3LYP/cc-pVTZ and MP2/6-31G(d) levels is 12–21 kcal mol^{-1} higher than the strain energy of three cyclobutanes (Table 2). The B3LYP value after ZPE corrections (82.0 kcal mol^{-1}) differs somewhat from the experimental value (97 kcal mol^{-1}), whereas the MP2 energy (93.5 kcal mol^{-1}) agrees better. Several computational studies have been devoted to C_{bh}–C_{bh} bond breakage in **4a**.[62–64] Experimentally, the barrier has been determined as 22 kcal mol^{-1},[32] and CASMP2/6-31G(d)//CASSCF-(8,8)/6-31G(d) calculations by Davidson gave a value of 17.5 kcal mol^{-1} including ZPE corrections.[62] This correlates with the short half-life of 28 min displayed by [2.2.2]propellan-2-amide at room temperature,[33] although the [2.2.2]propellanes of Lemal et al. have considerably longer lifetimes.[36] Davidson also concluded that spin-unrestricted DFT gives comparable energies to CASSCF.[62] Our B3LYP/6-31G(d) calculations reproduce his earlier result that the closed-shell state, with a doubly occupied σ*(C_{bh}–C_{bh}) orbital and a dissociated C_{bh}–C_{bh} bond, is 3.9 kcal mol^{-1} below the C_{bh}–C_{bh} bonded structure of **4a**. We now find that the dissociated structure is a second-order saddle point for the degenerate rearrangement between three 1,4-dimethylenecyclohexanes.

With C_{bh}-C_{bh}-C and C-C_{bh}-C angles of 90.6 and 120°, the bridgehead atoms of **4a** are sp^2-hybridized, and the C_{bh}–C_{bh} bond is formed by overlap of two 2p(C_{bh}) AOs. However, the C–C bonds of the ethylene tethers are longer and possibly weaker than the C_{bh}–C_{bh} bond (Figure 9). The MP2/6-31G(d) electron densities at the bond critical points are also lower for the peripheral bonds than for the central one ($\rho(r_b) = 1.557$ versus 1.768 e Å^{-3}), with lower bond orders for the former ($n = 0.91$ versus 1.14).[65] Thus, decomposition of **4a** into 1,4-dimethylenecyclohexane could possibly start by breakage of an ethylene tether instead of the C_{bh}–C_{bh} bond.

Descending Group 14, the C_{2h}-symmetric 1,4-dimethylene-1,4-dimetallacyclohexanes are higher in energy than the singlet biradicals **4b–4d** by 10.4, 22.5, and 45.1 kcal mol^{-1} at the PMP2/6-31G(d)(LANL2DZd) level. The corresponding (U)B3LYP/6-31G(d)(LANL2DZd) energies are somewhat lower (−1.5, 14.4, and 38.4 kcal mol^{-1}). When compared to oligomerization, rearrangement of **4c** and **4d** to the 1,4-dimethylene-1,4-dimetallacyclohexane is therefore unlikely, whereas it possibly could occur for **4b**. However, oligomerization of the biradicals **4b–4d** should be rapid, because dimer formation leads to energy gains of 73.4 (**4b**), 62.2 (**4c**), and 50.6 kcal mol^{-1}(**4d**) at the UB3LYP/6-31G(d)(LANL2DZd) level. Thus, none of **4b–4d** will be observable except at cryogenic temperatures.

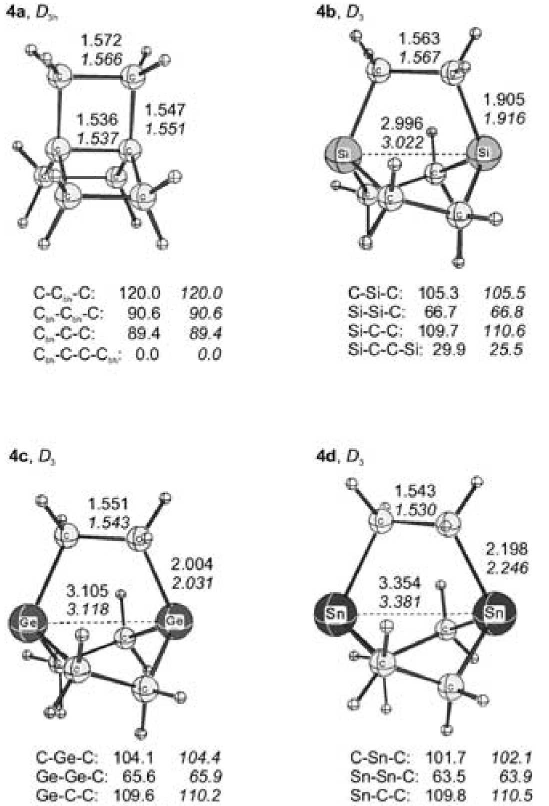

Figure 9. Optimal structures of **4a–4d** at the MP2/6-31G(d)(LANL2DZd) (normal print) and B3LYP/cc-pVTZ(SDB) (italics) levels.

As the Sn–Sn distance in **4d** is only about 0.5 Å longer than a regular Sn–Sn bond, one could expect that a stable closed-shell structure exists. However, when **4d** is constrained at the Sn–Sn distance of $H_3Sn–SnH_3$ (2.84 Å), it is destabilized by 15.8 kcal mol^{-1} at the MP2/6-31G(d)-(LANL2DZd) level, and only the biradical minimum could be found. It is noteworthy that the M–M bond lengths in 1,2-dimetallacyclobutanes (1.545 (M = C), 2.313 (M = Si), 2.461 (M = Ge), and 2.809 Å (M = Sn) at the MP2/6-31G(d)-(LANL2DZd) level) are similar to those of the corresponding M_2H_6 compounds (Table 1), but in the 1,4-digermabicyclo[2.2.0]hexane, Ohtaki and Ando found a long Ge–Ge bond which is about 0.05 Å longer than that calculated now for Ge_2H_6.[66] With a third ethylene tether, the strain exceeds the M–M bond strength. For instance, when the Sn–Sn bond is kept at normal distance in closed-shell **4d** the strain is 86 kcal mol^{-1} at the MP2/6-31G(d)-(LANL2DZd) level, which is larger than the homolytic dissociation energy of an Sn–Sn single bond, for example, 61.3 kcal mol^{-1} in $H_3Sn–SnH_3$ (CCSD(T) level with an extensive basis set).[67]

Considering that **4b**–**4d** are biradicals whereas 1,6-disilabicyclo[4.4.4]propellane is persistent at ambient temperature, the 1,5-dimetalla[3.3.3]propellanes (**6**) hold intricate positions. Their stabilities and those of the 1,5-dimetallabicyclo[3.3.3]undecanes (**5**) were probed next.

1,5-Dimetallabicyclo[1.1.1]undecanes (5): According to X-ray crystallography, bicyclo[3.3.3]undecane (**5a**) has C_{3h} symmetry,[68] but a C_s-symmetric conformer also exists that is less stable than the former by 7.5 kcal mol^{-1} at the MP2/6-31G(d) level. The C_s-symmetric conformers of **5b**–**5d** have relative energies of 3.1, 2.6, and 1.4 kcal mol^{-1} at the MP2/6-31G(d)(LANL2DZd) level.

As can be seen in Figure 10, **5a** is the most strained of **5a**–**5d**, and earlier measurements of heat of formation support its elevated strain.[69] The heavier analogues are only 50 % or less strained. The trend in strain energy when descending the Group is thus different from that in 1,4-dimetallabicyclo[2.2.2]octanes, and the reason for the particular strain in **5a** can be found in the C-C-C angles of the tethers, which are less distorted in **5b**–**5d** than in **5a** (Figure 11). Eight-membered rings are generally strained, and more so in **5a** than in the heavier analogues, because the energy released is larger in **5a** than in **5b**-**5d** (4.3 vs 0.6–0.4 kcal mol^{-1} at the MP2/6-31G(d)(LANL2DZd) level) when one cyclooctane ring in **5** goes from the geometry it adopts in **5** to the closest relaxed conformer.

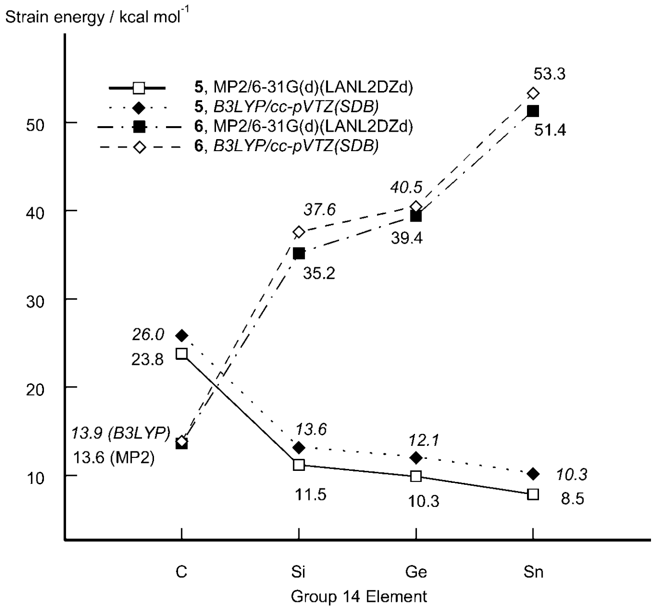

Figure 10. Homodesmotic strain energies of **5a**–**5d** and **6a**–**6d** at the B3LYP/cc-pVTZ(SDB) and MP2/6-31G(d)(LANL2DZd) levels.

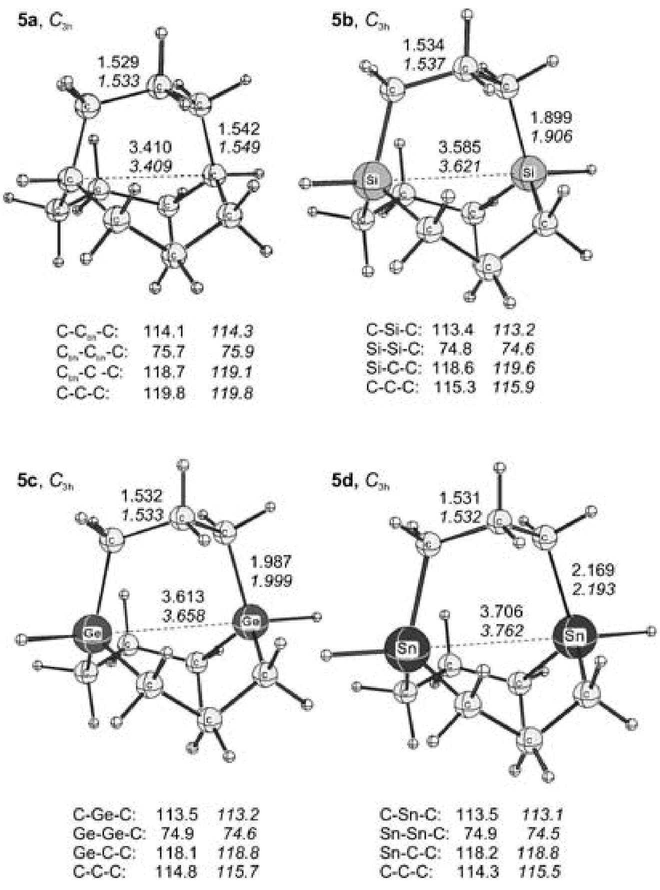

Figure 11. Optimal geometries of **5a**–**5d** at the MP2/6-31G(d)-(LANL2DZd) (normal print) and B3LYP/cc-pVTZ(SDB) (italics) levels.

1,5-Dimetalla[3.3.3]propellanes (6): The corresponding propellanes also have two conformers, of which the C_{3h}-symmetric conformers are more stable than their C_s-symmetric counterparts by 3.6 (**6a**), 0.9 (**6b**), 0.7 (**6c**), and 0.5 kcal mol^{-1} (**6d**) at the MP2/6-31G(d)(LANL2DZd) level. The most stable conformer of **6a** has a strain energy of 13.6 kcal mol^{-1} at the MP2/6-31G(d) level, that is, 12 kcal mol^{-1} lower than **5a**, although the $C_{bh}–C_{bh}$ bond of **6a** is about 0.06 Å longer than in ethane. The bridgehead C atoms are not inverted, and all C-C-C angles of the tethers are close to the tetrahedral angle (Figure 12). The homodes-

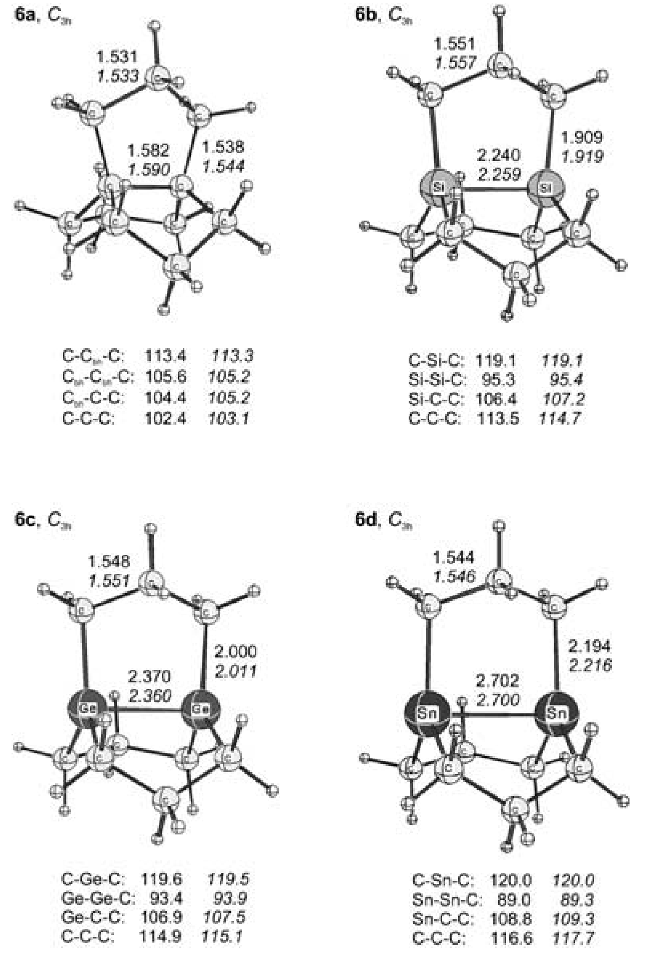

Figure 12. Optimal geometries of **6a**–**6d** at the MP2/6-31G(d)-(LANL2DZd) (normal print) and B3LYP/cc-pVTZ(SDB) (italics) levels.

motic strain of **6a** is 9.5 kcal mol^{-1} less than the combined strain of three cyclopentanes (Table 2), and distortion of a cyclopentane ring from its ideal geometry to that in **6a** costs merely 0.3 kcal mol^{-1} at the MP2/6-31G(d) level. Laidig found that hydrocarbon branching leads to stabilization, as it brings the atoms of a molecule closer and increases stabilizing interatomic interactions,[70] in agreement with findings that neopentane has a lower heat of formation than *n*-pentane by 4.4 kcal mol^{-1} at the MP2/6-31G(d,p) level and 3.6 ±0.2 kcal mol^{-1} according to experiment.[71,72] Similarly, the quaternary carbon atoms of **6a** provide stabilization compared to three cyclopentanes.

Whereas the C$_{bh}$–C$_{bh}$ distance in **6a** is longer than in ethane, the opposite applies to the M–M bonds in **6b**–**6d** when compared to the M–M bonds of M_2H_6 (Table 1), and M–M bond shortening is also found in **7b**–**7d**. The shortening of the M–M bonds in **6** and **7**, when compared to the M–M bonds in H_3M–MH_3, also increase as one goes from M = Si to Sn (Table 1). A similar bond shortening, yet smaller than in **6b**, was observed in the 1,6-disila[4.4.4]propellane of Tamao, Noro, and Kumada (Si–Si 2.295 Å),[7b] but not in the 3,7,10-trithiaoctasila[3.3.3]propellane of Herzog and Rheinwald (Si–Si 2.349 Å).[6] The mismatch in lengths between the propylene tethers and the M–M bonds become more pronounced as one goes down the Group, as is reflected in gradual M–M bond shortening, sp^2 hybridization of the M atoms, and widening of the C-C-C valence angles of the propylene tethers (Figure 12).

As a result of the successively more distorted structures, **6b**, **6c**, and **6d** are 16.6, 21.4, and 30.4 kcal mol^{-1} more strained than the three 1,2-dimetallacyclopentanes at the MP2/6-31G(d)(LANL2DZd) level, and the 1,5-dimetalla[3.3.3]propellanes is the only compound class for which a large increase in strain is observed on going down the Group (Figure 9). This increase in strain, combined with the gradually more planar structure around the M atoms, should facilitate M–M bond rupture. Similar to the 1,3-dimetalla[1.1.1]propellanes, the M–M bonds are also more polarizable on going down the Group ($\alpha_{zz}=1.51$ (**6a**), 1.98 (**6b**), 2.14 (**6c**), and 2.81×10^{-23} cm^{-3} (**6d**) at the B3LYP/6-31G(d)-(LANL2DZd) level), and the heavier [3.3.3]propellane becomes increasingly more strained than the analogous 1,5-dimetallabicyclo[3.3.3]undecane. All these effects will promote oligomerization. In this regard, it is notable that the strain of 1,6-disila[4.4.4]propellane is 15.6 kcal mol^{-1} at the MP2/6-31G(d)(LANL2DZd) level, that is, similar to that of **6a** but less than half that of **6b**.

A low relative energy of the biradical with a dissociated M–M bond will promote oligomerization, and the singlet biradical is of lowest energy for **6d** (10.3 and 9.7 kcal mol^{-1} at the (U)B3LYP/6-31G(d)(LANL2DZd) and PMP2/6-31G(d)(LANL2DZd) levels). The corresponding biradicals of **6b** and **6c** with dissociated M–M bonds are higher in energy (45.1 and 31.6 kcal mol^{-1} at the (U)B3LYP/6-31G(d)-(LANL2DZd) level, and 51.0 and 31.9 kcal mol^{-1} at the PMP2/6-31G(d)(LANL2DZd)//(U)B3LYP/6-31G(d)-(LANL2DZd) level). Consequently, unimolecular dissociation to the biradical should not occur at ambient temperature for **6b** and **6c**, but it should occur easily for **6d**. Furthermore, the electron densities at the Si–Si bond critical points of **6b** and 1,6-disilabicyclo[4.4.4]propellane (0.75 and 0.71 e Å^{-3}, respectively, at the B3LYP/6-31G(d) level) are slightly higher than those of the Si–Si bonds in Si_2H_6 and Si_2Me_6 (0.63 and 0.64 e Å^{-3}), and this supports our conclusion on strong Si–Si bonding in **6b**.

Two different dimerization mechanisms exist (Scheme 4). A stepwise mechanism initiated by formation of a biradical monomer through M–M bond dissociation and its subsequent attack on a second closed-shell monomer, and a mechanism in which two closed-shell monomers approach each other side-on, similar to dimerization of **2a**–**2d**. For **6d** dimerization is favorable because the singlet biradical dimer of **6d** lies 31.8 kcal mol^{-1} below two monomeric **6d** at the (U)B3LYP/6-31G(d)(LANL2DZd) level. Oligomerization should proceed stepwise but rapidly, because **6d** splits into a biradical via a transition state of 11.0 kcal mol^{-1}, and the addition of this biradical to a closed-shell **6d** proceeds without a barrier at the UB3LYP/6-31G(d)(LANL2DZd) level. Thus, **6d** will not be stable; the biradical monomer is acces-

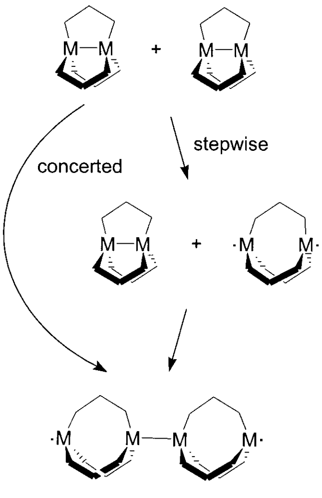

Scheme 4. Pathways for dimerization of **6**.

sible, and its reaction with a second closed-shell monomer initiates oligomerization.

The situation is more promising for **6c** and **6b**, because the dimers are less stable than two closed-shell monomers by 3.7 and 25.9 kcal mol^{-1}, respectively. The PMP2/6-31G(d)-(LANL2DZd)//UB3LYP/6-31G(d)(LANL2DZd) energies differ by at most 4 kcal mol^{-1} from the UB3LYP results. Dimerization of **6b** and **6c** by the stepwise mechanism is not likely, as the monomeric biradicals are too high in energy, and the concerted pathway would instead be followed. This pathway for dimerization of **6c** requires 23.7 kcal mol^{-1} at the UB3LYP/6-31G(d)(LANL2DZd) level, that is, monomeric **6c** will not be indefinitely stable at ambient temperature. When the biradical dimer of **6c** has formed, it is likely that its further oligomerization proceeds rapidly and irreversibly. Formation of the singlet biradical trimer of **6c** is a favorable process, because 18.4 kcal mol^{-1} is gained over three separate closed-shell monomers at the UB3LYP/6-31G(d)-(LANL2DZd) level. At the same level of computation, formation of the biradical dimer of **6b** by the concerted pathway proceeds via a transition state at 43.6 kcal mol^{-1}, which effectively hinders dimerization of this species, so that it should exist as a monomer at ambient temperature. It is only with the biradical tetramer of **6b** that energy is gained relative to the separate monomers (−15.3 kcal mol^{-1} at the UBLYP/6-31G(d)(LANL2DZd) level), and this lends further support to the existence of **6b** as a monomer. It should also be resistant to moisture, because 32.8 kcal mol^{-1} is needed to reach the transition state for hydrolytic cleavage of a Si–C bond (Figure 13).

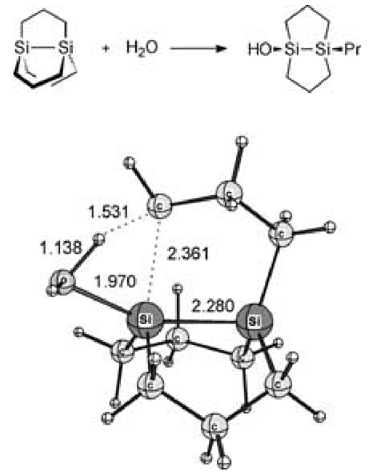

Figure 13. Transition-state structure for addition of H_2O to **6b**, calculated at the B3LYP/6-31G(d)(LANL2DZd) level. Distances in Å.

Generalizations and Outlook for Future Synthesis

None of the heavy 1,(*n*+2)-dimetallabicyclo[*n.n.n*]alkanes are excessively strained, and those with $n=1$ and 3 are even less strained than the all-carbon bicyclo[*n.n.n*]alkanes that already were synthesized. From the perspective of ring strain, the 1,(*n*+2)-dimetallabicyclo[*n.n.n*]alkanes are realistic synthetic targets, even though the 1,3-dimetallabicyclo-[1.1.1]pentanes become gradually more prone to hydrolysis as the Group is descended.

The situation is different for the 1,(*n*+2)-dimetallabicyclo-[*n.n.n*]propellanes. Only the 1,3-dimetalla[1.1.1]propellanes are less strained than the all-carbon propellane, yet they will not be of high stability. The increased M–M bond polarizability of the propellanes as one descends the Group promotes oligomerization, and this is critical for 1,3-dimetalla-[1.1.1]propellanes, for which the M–M distances in analogous dimetalla[1.1.1]propellanes and dimetallabicyclo-[1.1.1]pentanes are similar when M = Si–Sn. CASSCF calculations on the formation of dimeric biradicals from **2a** and **2b** reveal essential differences in their first oligomerization steps. In **2a**, the C_{bh}–C_{bh} bond has a bond order of 0.7,[59] and formation of the biradical dimer is thermodynamically unfavorable. In contrast, the Si–Si bond electron density in **2b** is diffuse and easily polarized, and this compound is neither thermodynamically nor kinetically stable toward dimerization, as there is almost no barrier for this process. Because of less relief in strain in the dimerizations of **2c** and **2d** than of **2b**, the biradical dimers of these compounds are less stable than two monomers, but **2c** and **2d** should still be more apt to oligomerize than **2a**. Extensive steric bulk caused by further substitution at the methylene bridges may prevent the species **2b**–**2d** from oligomerization.

With longer tethers ($n=2$ or 3) there is a mismatch between the tether and the optimal M–M bond length. For **4b**–**4d** the strengths of the M–M bonds do not compensate the high strain imposed by the tethers at closed-shell M–M bonded structures, and these compounds have biradical ground states. For **6**, the mismatch between optimal M–M bond and tether lengths becomes larger as one descends the Group; the M atoms go from sp^3 to sp^2 hybridization, and the M–M bonds gradually shorten. The homolytic Sn–Sn bond dissociation energy of **6d** is low as a result of the inverted character of this bond, and this compound will rapidly oligomerize. Only propellane **6b** should be truly persistent at ambient temperature, and it is most likely also unreactive to moisture.

The species considered by us as realistic synthetic targets may still be synthetically challenging due to intrinsic difficulties in their preparation, for example, low stability of intermediates. Because of the alkane tethers our investigated systems should be more stable to hydrolysis than small heavy bicycloalkanes with for example, −S− or −Se− tethers,[26] even though **1d** will rapidly be hydrolyzed. Oligomers based on **1b**–**1d** should be thermally inert, since the individual monomers are less strained than those of staffanes, and the latter compounds are robust at ambient temperatures. In the oligomers of **1b**–**1d** the M atoms will be at similar distances regardless whether they are formally bonded or not. This should allow for good coupling between the M atoms along the chain, possibly enabling a novel type of through-space σ-conjugated wires with interesting and useful optoelectronic properties. Investigations of such species will be reported in the near future.

Acknowledgements

Dr. Joshua R. Smith and Dr. Ahmed M. El-Nahas are thanked for discussions on the project. Financial support from the Swedish Research Council (Vetenskapsrådet), and a generous allotment of computer time from the National Supercomputer Center (NSC) in Linköping, Sweden, are gratefully appreciated.

---

[1] T. Iwamoto, D. Yin, C. Kabuto, M. Kira, *J. Am. Chem. Soc.* **2001**, *123*, 12730.

[2] K. B. Wiberg, *Acc. Chem. Res.* **1984**, *17*, 379.

[3] A. Schnepf, *Angew. Chem.* **2004**, *116*, 680; *Angew. Chem. Int. Ed.* **2004**, *43*, 664.

[4] K. B. Wiberg, F. H. Walker, *J. Am. Chem. Soc.* **1982**, *104*, 5239.

[5] a) L. R. Sita, R. D. Bickerstaff, *J. Am. Chem. Soc.* **1989**, *111*, 6454; b) L. R. Sita, I. Kinoshita, *J. Am. Chem. Soc.* **1990**, *112*, 8839.

[6] U. Herzog, G. Rheinwald, *Eur. J. Inorg. Chem.* **2001**, 3107.

[7] a) K. Tamao, M. Kumada, A. Noro, *J. Organomet. Chem.* **1971**, *31*, 169; b) D. Casher, H. Tsuji, A. Sano, M. Katkevics, A. Toshimitsu, K. Tamao, M. Kubota, T. Kobayashi, C. H. Ottosson, D. E. David, and J. Michl, *J. Phys. Chem. A* **2003**, *107* , 3559.

[8] H. Grützmacher, F. Breher, *Angew. Chem.* **2002**, *114*, 4178; *Angew. Chem. Int. Ed.* **2002**, *41*, 4006.

[9] S. Nagase, *Acc. Chem. Res.* **1995**, *28*, 469.

[10] W. Kutzelnigg, *Angew. Chem.* **1984**, *96*, 262; *Angew. Chem. Int. Ed. Engl.* **1984**, *23*, 272.

[11] M. D. Levin, P. Kaszynski, J. Michl, *Chem. Rev.* **2000**, *100*, 169.

[12] K. B. Wiberg. D. S. Connor, *J. Am. Chem. Soc.* **1966**, *88*, 4437.

[13] M. Barfield, E. W. Della, P. E. Pigou, S. R. Walter, *J. Am. Chem. Soc.* **1982**, *104*, 3549.

[14] B. Maillard, J. C. Walton, *J. Chem. Soc. Chem. Commun.* **1983**, 900.

[15] W. Adcock, A. R. Krstic, *Tetrahedron Lett.* **1992**, *33*, 7397.

[16] A. J. McKinley, P. N. Ibrahim, V. Balaji, J. Michl, *J. Am. Chem. Soc.* **1992**, *114*, 10631.

[17] W. Adcock, G. T. Binmore, A. R. Krstic, J. C. Walton, J. Wilkie, *J. Am. Chem. Soc.* **1995**, *117*, 2758.

[18] E. W. Della, C. A. Grob, D. K. Taylor, *J. Am. Chem. Soc.* **1994**, *116*, 6159.

[19] W. Adcock, A. R. Krstic, *Magn. Reson. Chem.* **1997**, *35*, 663.

[20] W. Adcock, A. V. Blokhin, G. M. Elsey, N. H. Head, A. R. Krstic, M. D. Levin, J. Michl, J. Munton, E. Pinkhassik, M. Robert, J.-M. Savéant, A. Shtarev, I Stibor, *J. Org. Chem.* **1999**, *64*, 2618.

[21] a) R. West, A. Indriksons, *J. Am. Chem. Soc.* **1972**, *94*, 6110; b) H. Bock, W. Kaim, M. Kira, R. West, *J. Am. Chem. Soc.* **1979**, *101*, 7667.

[22] R. Fischer, T. Konopa, S. Ully, J. Baumgartner, C. Marschner, *J. Organomet. Chem.* **2003**, *685*, 79.

[23] U. Herzog, G. Rheinwald, *Organometallics* **2001**, *20*, 5369.

[24] L. R. Sita, I. Kinoshita, *J. Am. Chem. Soc.* **1991**, *113*, 5070.

[25] Y. Kabe, T. Kawase, J. Okada, O. Yamashita, M. Goto, S. Masamune, *Angew. Chem.* **1990**, *102*, 823; *Angew. Chem. Int. Ed. Engl.* **1990**, *29*, 794.

[26] a) N. Choi, K. Asano, W. Ando, *Organometallics* **1995**, *14*, 3146; b) H. Yoshida, Y. Takahara, T. Erata, W. Ando, *J. Am. Chem. Soc.* **1992**, *114*, 1098.

[27] M. Takahashi, K. Hatano, Y. Kawada, G. Koga, N. Tokitoh, R. Okazaki, *J. Chem. Soc. Chem. Commun.* **1993**, 1850.

[28] a) N. Rot, T. Nijbacker, R. Kroon, F. J. J. de Kanter, F. Bickelhaupt, M. Lutz, A. L. Spek, *Organometallics* **2000**, *19*, 1319; b) M. A. Dam, F. J. J. Kanter, F. Bickelhaupt, W. J. J. Smeets, A. L. Spek, J. Fornies-Camer, C. Cardin, *J. Organomet. Chem.* **1998**, *550*, 347; c) M. A. Dam; M. W. J. Hoogervorst, F. J. J. de Kanter, F. Bickelhaupt, A. L. Spek, *Organometallics* **1998**, *17*, 1762; d) M. A. Dam; O. S. Akkerman, F. J. J. de Kanter, F. Bickelhaupt, N. Veldman, A. L. Spek, *Chem. Eur. J.* **1996**, *2*, 1139.

[29] D. B. Kitchen, J. E. Jackson, L. C. Allen, *J. Am. Chem. Soc.* **1990**, *112*, 3408.

[30] K. B. Wiberg, F. H. Walker, *J. Am. Chem. Soc.* **1982**, *104*, 5239.

[31] K. B. Wiberg, D. S. Connor, G. M. Lampman, *Tetrahedron Lett.* **1964**, *5*, 531.

[32] P. E. Eaton, G. H. Temme, *J. Am. Chem. Soc.* **1973**, *95*, 7508.

[33] F. W. Semmler, K. Bartelt, *Ber. Dtsch. Chem. Ges.* **1907**, *40*, 4844.

[34] N. Takaishi, Y. Inamoto, K. Tsuchihashi, K. Yashima, K. Aigami, *J. Org. Chem.* **1975**, *40*, 2929.

[35] a) M. Doyle, W. Parker, P. A. Gunn, J. Martin, D. D. Macnicol, *Tetrahedron Lett.* **1970**, *11*, 3619; b) N. J. Leonard, J. C. Coll, *J. Chem. Soc.* **1970**, *92*, 6685.

[36] a) Y. Zhang, J. Smith, D. M. Lemal, *J. Am. Chem. Soc.* **1996**, *118*, 9454; b) Y. He, C. P. Junk, J. J. Cawley, D. M. Lemal, *J. Am. Chem. Soc.* **2003**, *125*, 5590.

[37] Gaussian 03, Revision B.05. M. J. Frisch, G. W. Trucks, H. B. Schlegel, G. E. Scuseria, M. A. Robb, J. R. Cheeseman, J. A. Montgomery, Jr., T. Vreven, K. N. Kudin, J. C. Burant, J. M. Millam, S. S. Iyengar, J. Tomasi, V. Barone, B. Mennucci, M. Cossi, G. Scalmani, N. Rega, G. A. Petersson, H. Nakatsuji, M. Hada, M. Ehara, K. Toyota, R. Fukuda, J. Hasegawa, M. Ishida, T. Nakajima, Y. Honda, O. Kitao, H. Nakai, M. Klene, X. Li, J. E. Knox, H. P. Hratchian, J. B. Cross, C. Adamo, J. Jaramillo, R. Gomperts, R. E. Stratmann, O. Yazyev, A. J. Austin, R. Cammi, C. Pomelli, J. W. Ochterski, P. Y. Ayala, K. Morokuma, G. A. Voth, P. Salvador, J. J. Dannenberg, V. G. Zakrzewski, S. Dapprich, A. D. Daniels, M. C. Strain, O. Farkas, D. K. Malick, A. D. Rabuck, K. Raghavachari, J. B. Foresman, J. V. Ortiz, Q. Cui, A. G. Baboul, S. Clifford, J. Cioslowski, B. B. Stefanov, G. Liu, A. Liashenko, P. Piskorz, I. Komaromi, R. L. Martin, D. J. Fox, T. Keith, M. A. Al-Laham, C. Y. Peng, A. Nanayakkara, M. Challacombe, P. M. W. Gill, B. Johnson, W. Chen, M. W. Wong, C. Gonzalez, J. A. Pople, Gaussian, Inc., Pittsburgh, PA, **2001**.

[38] A. D. Becke, *J. Chem. Phys.* **1993**, *98*, 1372.

[39] P. C. Hariharan, J. A. Pople, *Theor. Chim. Acta* **1973**, *28*, 213.

[40] a) P. J. Hay, W. R. Wadt, *J. Chem. Phys.* **1985**, *82*, 270; b) W. R. Wadt, P. J. Hay, *J. Chem. Phys.* **1985**, *82*, 284; c) P. J. Hay, W. R. Wadt, *J. Chem. Phys.* **1982**, *82*, 299.

[41] C. E. Check, T. O. Faust, J. M. Bailey, B. J. Wright, T. M. Gilbert, L. S. Sunderlin, *J. Phys. Chem. A* **2001**, *105*, 8111.

[42] J. M. L. Martin, A. Sundermann, *J. Chem. Phys.* **2001**, *114*, 3408.

[43] R. Bauernschmitt, R. Ahlrichs, *J. Chem. Phys.* **1996**, *104*, 9047.

[44] T. J. Lee, P. R. Taylor, *Int. J. Quant. Chem.* **1989**, *S23*, 199.

[45] R. F. W. Bader, *Chem. Rev.* **1991**, *91*, 893.

[46] AIM2000, Version 1.0, F. Biegler-König, D. Bayles, J. Schönbohm, University of Applied Sciences, Bielefeld, Germany, **2000**.

[47] P. George, M. Trachtman, C. W. Bock, A. M. Brett, *Tetrahedron* **1976**, *32*, 317.

[48] P. N. Skancke, J. F. Liebman, *Int. J. Quantum Chem.* **1996**, *58*, 707–715.

[49] K. B. Wiberg, *J. Am. Chem. Soc.* **1983**, *105*, 1227.

[50] J. F. Chiang, S. H. Bauer, *J. Am. Chem. Soc.* **1970**, *92*, 1614.

[51] A. Bondi, *J. Phys. Chem.* **1964**, *68*, 441. Only van der Waals radii from Pauling's approximation (r_b) and based on half the de Broglie wavelengths ($\lambda_B/2$) are available for C, Si, Ge, and Sn. The values are as follows: C ($r_b=1.53$, $\lambda_B/2=1.82$), Si ($r_b=1.93$, $\lambda_B/2=2.15$), Ge ($r_b=1.98$, $\lambda_B/2=2.19$), Sn ($r_b=2.16$, $\lambda_B/2=2.27$).

[52] a) S. Nagase, T. Kudo, *Organometallics* **1987**, *6*, 2456; b) S. Nagase, T. Kudo, T. Kurakake, *J. Chem. Soc. Chem. Commun.* **1988**, 1063; c) S. Nagase, T. Kudo, *Organometallics* **1988**, *7*, 2534.

[53] O. Jarosch, R. Walsh, G. Szeimies, *J. Am. Chem. Soc.* **2000**, *122*, 8490.

[54] a) A. G. Brook, H. J. Wessely, *Organometallics* **1985**, *4*, 1487; b) T. Tsumuraya, S. Sato, W. Ando, *Organometallics* **1990**, *9*, 2061.

[55] L. Hedberg, K. Hedberg, *J. Am. Chem. Soc.* **1985**, *107*, 7257.

[56] O. Schafer, M. Allan, G. Szeimies, M. Sanktjohanser, *J. Am. Chem. Soc.* **1992**, *114*, 8180.

[57] K. Jug, A. Poredda, *J. Am. Chem. Soc.* **1991**, *113*, 761.

[58] K. A. Nguyen, M. T. Carrol, M. S. Gordon, *Polyhedron* **1991**, *10*, 1247.

[59] W. Adcock, M. J. Brunger, C. I. Clark, I. E. McCarthy, M. T. Michalewicz, W. von Niessen, W. Weigold, D. A. Winkler, *J. Am. Chem. Soc.* **1997**, *119*, 2896.

[60] K. A. Nguyen, M. T. Carroll, M. S. Gordon, *J. Am. Chem. Soc.* **1991**, *113*, 7924.

[61] The norms of the singles amplitude vectors are 0.011 (**2a**), 0.012 (**2b**), 0.012 (**2c**), and 0.014 (**2d**), that is, significantly below the threshold value of 0.02 for multiconfigurational character.

[62] E. R. Davidson, *Chem. Phys. Lett.* **1998**, *284*, 301.

[63] D. Feller, E. R. Davidson, *J. Am. Chem. Soc.* **1987**, *109*, 4133.

[64] M. D. Newton, J. M. Schulman, *J. Am. Chem. Soc.* **1972**, *94*, 4391.

[65] The bond order n is given by the equation $n=\exp[a(\rho_b-b)]$, where ρ_b is the electron density at the bond critical point and the two constants a and b were determined from ρ_b(ethane) and ρ_b(ethene) at the MP2/6-31G(d) level to be 1.647 and 2.292 e Å^{-3}.

[66] T. Ohtaki, W. Ando, *Organometallics* **1996**, *15*, 3103.

[67] M. Kaupp, B. Metz, H. Stoll, *Angew. Chem.* **2000**, *112*, 4780; *Angew. Chem. Int. Ed.* **2000**, *39*, 4607.

[68] P. Murray-Rust, J. Murray-Rust, C. I. F. Watt, *Tetrahedron* **1980**, *36*, 2799.

[69] W. Parker, W. V. Steel, I. Watt, *J. Chem. Thermodyn.* **1977**, *9*, 307.

[70] K. E. Laidig, *J. Phys. Chem.* **1991**, *95*, 7709.

[71] K. B. Wiberg, *J. Org. Chem.* **1991**, *56*, 544.

[72] Enthalpies of formation at 298 K from J. B. Pedley, R. D. Naylor, S. P. Kirby, *Thermochemical Data of Organic Compounds*, 2nd ed., Chapman and Hall, London **1986**. Vibrational frequencies from L. M. Sverdlov, M. A. Kovner, E. P. Krainov, *Vibrational Spectra of Organic Molecules*, Halsted Press, New York, **1974**.

Received: January 14, 2005